Bioconjugate Chemistry

Article

pubs.acs.org/bc

Synthesis and Biological Evaluation of a Polyyne-Containing Sphingoid Base Probe as a Chemical Tool

Yun Mi Lee,[†] Chaemin Lim,[†] Hun Seok Lee,[†] Young Kee Shin,[†] Kyong-Oh Shin,[‡] Yong-Moon Lee,[‡] and Sanghee Kim*,[†]

[†]College of Pharmacy, Seoul National University, 1 Gwanak-ro, Gwanak-gu, Seoul 151-742, Korea

[‡]College of Pharmacy and MRC, Chungbuk National University, Cheongju 361-763, Korea

Supporting Information

ABSTRACT: The sphingolipid metabolites have emerged as a starting point for the development of novel therapeutics for many diseases. However, details of the functions and mechanisms of sphingolipids remain unknown. To better understand the roles of sphingolipids, chemical tools with unique biological and physicochemical properties are needed. In this regard, we previously reported the synthesis of sphingoid base analogues in which the carbon chains are restricted by triple bonds. Here, we have conjugated a fluorescent dye to the polyyne analogues of the sphingoid bases to generate optical probes. Like the parent polyyne-containing sphingoid base, the 7-nitrobenz-2-oxa-1,3-diazol-4-yl (NBD)-labeled triyne-sphingosine inhibited cancer cell growth far more effectively than did the corresponding sphingosine. NBD-triyne-sphingosine was rapidly incorporated into the cells and displayed broad cytoplasmic distribution. According to the results of a flow cytometric analysis, cancer cells fed with NBD-triyne-sphingosine showed significantly increased fluorescence intensity compared with the NBD-sphingosine treated cells. The metabolism of NBD-triyne-sphingosine was somewhat different from that of NBD-sphingosine. These results indicated that the incorporated rigid polyyne moiety in the sphingoid base altered the physicochemical properties of the sphingolipid, thereby affecting its biological behavior. The higher antiproliferative activity in the SRB assay and the significantly higher fluorescence intensity observed in the flow cytometric analysis are some of the interesting and distinct aspects of NBD-triyne-sphingosine compared to standard NBD-sphingosine probes. Thus, it is believed that the fluorescently labeled polyyne-containing sphingoid base developed in this study will be a useful chemical tool in sphingolipid research.

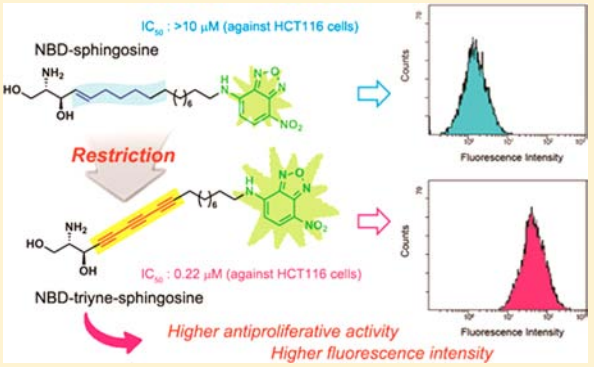

INTRODUCTION

Sphingolipids are a structurally diverse class of lipids that contain a sphingoid base as the backbone. They can be metabolically interconverted to one another through the action of enzymes. Different sphingolipids display different biological functions.[1−3] For example, sphingosine-1-phosphate (S1P) has anti-apoptotic and proliferative activity,[4−6] whereas the *N*-acylated sphingoid base, ceramide, displays the opposite effect.[7−9] Because the dynamic balance between the intracellular levels of ceramide and S1P determine a cell's fate, the concept of a ceramide/S1P rheostat was proposed[4] and serves as a conceptual starting point for the development of novel therapeutics from the sphingolipid metabolites and targets.[10−14] In the last few decades, extensive research has been devoted to the biological role of sphingolipids. However, there are still many important questions that remain unanswered about their specific regulatory mechanisms and functions.[1,2]

Sphingoid bases are long-chain aliphatic compounds that have a 2-amino-1,3-diol functionality within their structures. They are bioactive sphingolipids and also compose the chemical backbone of all sphingolipids. Sphingosine (**1**, Figure 1), the typical sphingoid base, has been known to induce apoptosis when added exogenously to cells.[7,15] Sphingosine is believed to play a role in apoptosis cooperatively and independently from the apoptotic signaling of ceramide.[16,17] Due to the interesting biological functions of sphingoid bases and their structural role as the principal backbone of sphingolipids, chemical modification of the structure of sphingoid bases has received considerable attention.[18−21] Most modifications have been carried out for two general purposes: (1) to unravel the biochemical functions of sphingolipids and (2) to confer drug-like properties.

Sphingoid bases are acyclic molecules; thus, they can adopt multiple conformations. We envisioned that the conformationally restricted analogs of sphingoid bases might be useful as a chemical tool to probe the biological functions of sphingolipids. In this regard, we previously reported the synthesis of polyyne-containing sphingoid bases of the general structures **2** and **3**

Received: December 21, 2012
Revised: July 22, 2013
Published: August 8, 2013

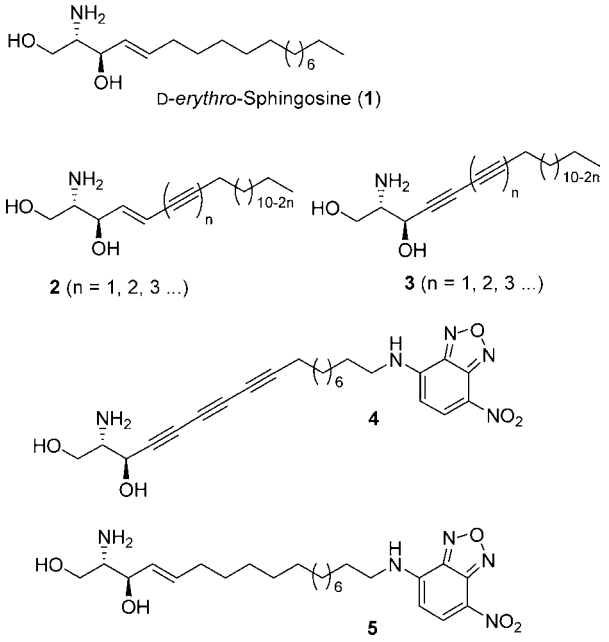

Figure 1. Chemical structures of sphingosine **1** and compounds **2**–**5**.

(Figure 1) via an iterative acetylene homologation sequence.[22] The incorporated rigid polyyne moiety in the sphingoid base was expected to alter the physicochemical properties of the sphingolipid, thereby affecting its biological behavior.[23]

In this article, we present the results of our efforts to develop polyyne-containing sphingoid bases as chemical tools. Because the polyyne analogues **2** and **3** lack distinctive spectroscopic signatures that are useful for the investigation of the biological functions of sphingolipids, we incorporated a 7-nitrobenz-2-oxa-1,3-diazol-4-yl (NBD) group at the terminus of the sphingosine backbone to yield the new fluorescently labeled sphingoid base **4**; we then conducted a chemical and biological evaluation of this new probe. A number of fluorescently labeled sphingolipids, including the NBD-sphingosine **5**, have been used in many areas as tools to elucidate the cellular modulation of sphingolipids.[24−33] Our NBD-polyyne-sphingosine **4** displayed notable differences in behavior compared with commercially available NBD-sphingosine **5**.

EXPERIMENTAL PROCEDURES

Chemistry. *General Methods.* All of the chemicals were reagent grade and used as purchased. All of the reactions were performed under an inert atmosphere of dry argon or nitrogen using distilled dry solvents. The reactions were monitored by TLC analysis using silica gel 60 F-254 TLC plates. Compounds were visualized by UV light (254 and 365 nm). Flash column chromatography was carried out on silica gel (230−400 mesh). Optical rotations were measured using a polarimeter set for sodium D light (589.3 nm). ^{1}H NMR (500 or 300 MHz) and ^{13}C NMR (125 or 75 MHz) spectra were recorded in δ units relative to the nondeuterated solvent as an internal reference. High-resolution mass spectra (HRMS) were recorded using fast atom bombardment (FAB) or chemical ionization (CI). UV/vis absorption and fluorescence spectra were recorded using HITACHI JP/U-3010 and JASCO FP-6500 instruments, respectively.

Synthesis of Compound 4. The synthetic route to prepare compound **4** is shown in Scheme 1. Preparation of bromodiyne **6** was performed according to literature procedures.[22]

Scheme 1. Synthesis of Polyyne-Containing Sphingoid Base Fluorescence Probe 4[a]

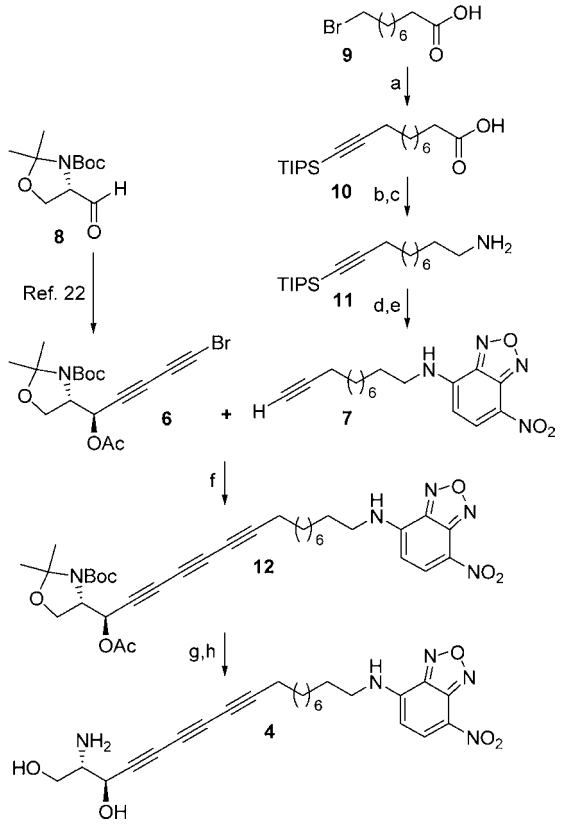

[a]Reagents and conditions: (a) TIPSA, *n*-BuLi, HMPA, Toluene, −78 to 0 °C, 1 h, 73%; (b) NMM, isobutyl chloroformate, THF, −20 °C, 0.5 h, then NH_3 solution in MeOH, RT, 12 h, 94%; (c) $LiAlH_4$, Et_2O, RT, 12 h, 83%; (d) NBD-Cl, Et_3N, DMF, RT, 2 h, 81%; (e) TBAF, THF, RT, 5 h, 99%; (f) $Pd(PPh_3)_2Cl_2$, *i*-Pr_2NH, CuI, THF, RT, 1 h, 59%; (g) K_2CO_3, MeOH, RT, 2 h; (h) TFA, CH_2Cl_2, H_2O, RT, 12 h, 69% (two steps).

Synthesis of 11-(Triisopropylsilyl)undec-10-ynoic Acid (10). *n*-BuLi (8.70 mL, 13.93 mmol, 1.6 M solution in hexane) was slowly added to a cooled (−78 °C) solution of (triisopropyl)acetylene (2.81 mL, 12.66 mmol) in THF (10 mL). After stirring for 30 min, a solution of bromo acid **9** (1.00 mL, 4.22 mmol) in THF (6 mL) and HMPA (4 mL) was slowly added over 10 min at −78 °C. After stirring for 30 min at −78 °C, the reaction mixture was slowly warmed to room temperature and quenched with saturated aqueous NH_4Cl solution. The mixture was diluted with EtOAc and washed with brine. The organic layer was dried over $MgSO_4$, filtered, and concentrated under reduced pressure. The residue was purified using silica gel column chromatography (hexane/EtOAc, 3:1, with 0.1% acetic acid) to give the acetylenic compound **10** (1.04 g, 73%) as a colorless oil: R_f = 0.4 (hexane/EtOAc, 4:1), ^{1}H NMR (300 MHz, $CDCl_3$) δ 0.99−1.08 (m, 21H), 1.26−1.44 (m, 8H), 1.47−1.54 (m, 2H), 1.61−1.66 (m, 2H), 2.24 (t, J = 6.9 Hz, 2H), 2.35 (t, J = 7.8 Hz, 2H); ^{13}C NMR (75 MHz, $CDCl_3$) δ 11.3 (3C), 18.6 (6C), 19.7, 24.6, 28.5, 28.7, 28.8,

dx.doi.org/10.1021/bc300684q | *Bioconjugate Chem.* 2013, 24, 1324−1331

29.0, 29.1, 34.1, 80.0, 109.1, 180.6; HRMS (FAB) calcd for $C_{20}H_{38}O_2SiNa$ ($[M+Na]^+$) 361.2539, found 361.2545.

Synthesis of 11-(Triisopropylsilyl)undec-10-yn-1-amine (11). Iso-butylchloroformate (0.57 mL, 4.43 mmol) was added to a cooled (−20 °C) solution of **10** (1.00 g, 2.95 mmol) and 4-methylmorpholine (0.49 mL, 4.43 mmol) in THF (30 mL). After stirring for 30 min at −20 °C, a solution of ammonia (2.42 mL, 8.85 mmol, ca. 7 N solution in methanol) was added. The reaction mixture was slowly warmed to 0 °C and stirred overnight. The mixture was diluted with EtOAc and washed with brine. The organic layer was dried over $MgSO_4$, filtered, and concentrated under reduced pressure. The residue was purified using silica gel column chromatography (hexane/EtOAc, 1:1) to give the amide (0.94 g, 94%) as a white waxy solid: R_f = 0.4 (hexane/EtOAc, 1:1), ^{1}H NMR (300 MHz, $CDCl_3$) δ 1.00−1.09 (m, 21H), 1.25−1.43 (m, 8H), 1.47−1.56 (m, 2H), 1.59−1.66 (m, 2H), 2.21−2.27 (m, 4H), 5.81 (br s, 2H); ^{13}C NMR (75 MHz, $CDCl_3$) δ 11.1 (3C), 18.5 (6C), 19.6, 25.4, 28.4, 28.6, 28.7, 29.0, 29.1, 35.8, 79.8, 109.1, 176.3; HRMS (FAB) calcd for $C_{20}H_{40}NOSi$ ($[M+H]^+$) 338.2879, found 338.2871.

$LiAlH_4$ (11.12 mL, 11.12 mmol, 1.0 M solution in THF) was slowly added to a cooled (0 °C) solution of amide (900 mg, 2.78 mmol) in diethyl ether (12 mL). The reaction mixture was warmed to room temperature, stirred overnight, cooled to 0 °C, and quenched by successive addition of water (0.4 mL), 15% NaOH (0.4 mL), and water (1.2 mL). The resulting suspension was warmed to room temperature, filtered through Celite, and eluted with diethyl ether. The resulting solution was carefully concentrated and the residue was purified using silica gel column chromatography (CH_2Cl_2/MeOH/NH_4OH, 10:1:0.1) to give the amine **11** (747 mg, 83%) as a colorless oil: R_f = 0.4 (CH_2Cl_2/MeOH, 10:1), ^{1}H NMR (300 MHz, CD_3OD) δ 1.04−1.09 (m, 21H), 1.30−1.35 (m, 8H), 1.48−1.50 (m, 6H), 2.26 (t, J = 6.3 Hz, 2H), 2.68 (t, J = 7.2 Hz, 2H); ^{13}C NMR (75 MHz, CD_3OD) δ 12.5 (3C), 19.2 (6C), 20.4, 28.0, 29.7, 29.9, 30.1, 30.6, 30.7, 33.4, 42.4, 80.7, 110.5; HRMS (CI) calcd for $C_{20}H_{42}NSi$ ($[M+H]^+$) 324.3087, found 324.3081.

Synthesis of 7-Nitro-*N*-(undec-10-ynyl)benzo[*c*][1,2,5]oxadiazol-4-amine (7). 7-Nitrobenzo-2-oxa-1,3-diazol-4-yl chloride (440 mg, 2.16 mmol) was added to a solution of amine **11** (700 mg, 2.16 mmol) and Et_3N (0.45 mL, 3.24 mmol) in DMF (22 mL) at room temperature. After stirring for 2 h at same temperature, the reaction mixture was diluted with water and extracted with EtOAc. The organic layer was dried over $MgSO_4$, filtered, and concentrated under reduced pressure. The residue was purified using silica gel column chromatography (hexane/EtOAc/CH_2Cl_2, 8:1:1) to give the fluorescent TIPS-acetylene compound (852 mg, 81%) as a dark yellow oil: R_f = 0.3 (hexane/EtOAc, 5:1), ^{1}H NMR (300 MHz, $CDCl_3$) δ 1.03−1.08 (m, 21H), 1.34−1.55 (m, 12H), 1.81 (m, 2H), 2.25 (t, J = 6.6 Hz, 2H), 3.48 (dd, J = 5.7, 12.9 Hz, 2H), 6.17 (d, J = 8.4 Hz, 1H), 8.50 (d, J = 8.7 Hz, 1H); ^{13}C NMR (75 MHz, $CDCl_3$) δ 11.1 (3C), 18.5 (6C), 19.6, 26.8, 28.37, 28.43, 28.6, 28.8, 29.0, 29.2, 44.0, 79.8, 98.5, 109.1 (2C), 123.2, 136.6, 143.8, 144.1; HRMS (CI) calcd for $C_{26}H_{43}N_4O_3Si$ ($[M+H]^+$) 487.3104, found 487.3109.

Tetrabutylammonium fluoride (43.75 mL, 43.75 mmol, 1.0 M solution in THF) was added to a solution of fluorescent TIPS-acetylene (850 mg, 1.75 mmol) in THF (80 mL) at room temperature. After stirring overnight at room temperature, the resultant mixture was quenched with saturated aqueous NH_4Cl solution and extracted with EtOAc. The organic layer was dried over $MgSO_4$, filtered, and concentrated under reduced pressure. The residue was purified using silica gel column chromatography (hexane/EtOAc, 4:1) to give the desilylated compound **7** (572 mg, 99%) as a red solid: R_f = 0.3 (hexane/EtOAc, 4:1), ^{1}H NMR (300 MHz, $CDCl_3$) δ 1.25−1.57 (m, 12H), 1.81 (m, 2H), 1.94 (t, J = 2.7 Hz, 1H), 2.18 (dt, J = 2.7, 7.2 Hz, 2H), 3.49 (dd, J = 6.0, 13.2 Hz, 2H), 6.17 (d, J = 8.7 Hz, 1H), 6.22 (br s, 1H), 8.49 (d, J = 8.4 Hz, 1H); ^{13}C NMR (75 MHz, $CDCl_3$) δ 18.3, 26.9, 28.4, 28.5, 28.6, 28.9, 29.1, 29.3, 44.0, 68.1, 84.6, 98.5, 124.0, 136.5, 143.8, 143.9, 144.3; HRMS (CI) calcd for $C_{17}H_{23}N_4O_3$ ($[M+H]^+$) 331.1770, found 331.1765.

Synthesis of (*S*)-*tert*-Butyl 4-((*R*)-1-acetoxy-16-(7-nitrobenzo[*c*][1,2,5]oxadiazol-4-ylamino)hexadeca-2,4,6-triynyl)-2,2-dimethyloxazolidine-3-carboxylate (12). Diisopropylamine (0.06 mL, 0.42 mmol) was added to a degassed solution of bromodiyne **6** (80 mg, 0.20 mmol), terminal acetylene **7** (73 mg, 0.22 mmol), $Pd(PPh_3)_2Cl_2$ (4 mg, 0.01 mmol), and CuI (1 mg, 0.01 mmol) in THF (3 mL). The reaction mixture was stirred for 1 h at room temperature and then quenched with saturated aqueous NH_4Cl solution. The reaction mixture was diluted with EtOAc, washed with brine, dried over $MgSO_4$, filtered, and concentrated under reduced pressure. The resulting residue was purified using silica gel column chromatography (hexane/EtOAc, 3:1) to give triyne **12** (77 mg, 59%) as a dark yellow waxy solid: R_f = 0.3 (hexane/EtOAc, 3:1); ^{1}H NMR (300 MHz, $CDCl_3$, mixture of rotamers) δ 1.23−1.54 (m, 27H), 1.76−1.87 (m, 2H), 2.10 (d, J = 3.9 Hz, 3H), 2.30 (t, J = 6.9 Hz, 2H), 3.49 (dd, J = 6.0, 13.2 Hz, 2H), 4.00−4.22 (m, 3H), 5.82−5.88 (m, 1H), 6.18 (d, J = 8.4 Hz, 1H), 6.40 (br s, 1H), 8.50 (d, J = 8.7 Hz, 1H); ^{13}C NMR (75 MHz, $CDCl_3$, rotamer 1/rotamer 2) δ 19.4, 20.9, 23.1, 24.4, 26.0, 26.7, 26.9, 27.8, 28.3, 28.5, 28.6, 28.8, 29.1, 44.0, 58.6/58.7, 59.5, 59.8, 63.2, 64.0/64.4, 64.6/64.9, 65.3/65.4, 71.6, 71.7/71.8, 78.2, 80.9/81.0, 81.6/81.8, 95.0, 98.5, 124.1, 136.5, 143.8, 143.9, 144.3, 169.5; HRMS (FAB) calcd for $C_{34}H_{43}N_5O_8Na$ ($[M+Na]^+$) 672.3009, found 672.3002.

Synthesis of (2*S*,3*R*)-2-Amino-18-(7-nitrobenzo[*c*][1,2,5]oxadiazol-4-ylamino)octadeca-4,6,8-triyne-1,3-diol (4). K_2CO_3 (5 mg, 0.04 mmol) was added to a solution of triyne **12** (16.2 mg, 0.02 mmol) in methanol (2 mL). After stirring for 2 h at room temperature, the reaction mixture was evaporated to remove the MeOH, diluted with EtOAc, washed with brine, dried over $MgSO_4$, and concentrated under reduced pressure. A solution of the resulting residue in CH_2Cl_2/TFA/H_2O (2:2:1, 0.1 M) was stirred for 12 h at room temperature. The reaction mixture was quenched with saturated $NaHCO_3$ solution and then extracted with EtOAc. The organic layer was washed with brine, dried over $MgSO_4$, filtered, and concentrated under reduced pressure. The residue was purified using silica gel column chromatography (CH_2Cl_2/MeOH, 8:1) to give **4** (18.9 mg, 69%) as a dark yellow solid: R_f = 0.25 (CH_2Cl_2/MeOH, 10:1); $[\alpha]^{25}_D$ −7.3 (c 0.6, CH_3OH); ^{1}H NMR (500 MHz, CD_3OD) δ 1.24−1.43 (m, 10H), 1.45−1.58 (m, 4H), 1.77 (dt, J = 7.3, 14.5 Hz, 2H), 2.31 (t, J = 7.0 Hz, 2H), 2.97 (dd, J = 5.4, 11.6 Hz, 1H), 3.51 (br s, 2H), 3.61 (dd, J = 6.4, 11.2 Hz, 1H), 3.68 (dd, J = 5.3, 11.2 Hz, 1H), 4.50 (d, J = 5.4 Hz, 1H), 6.30 (d, J = 8.9 Hz, 1H), 8.47 (d, J = 8.8 Hz, 1H); ^{13}C NMR (125 MHz, CD_3OD) δ 20.6, 28.8, 29.8, 30.1, 30.6, 30.7, 31.0, 31.2, 45.7, 59.2, 60.4, 63.6, 65.2, 65.4, 66.6, 72.4, 77.6, 83.3, 100.4, 123.6, 139.4, 146.3, 146.6, 147.5; HRMS (FAB) calcd for $C_{24}H_{30}N_5O_5$ ($[M+H]^+$) 468.2247, found 468.2253.

Biology. *Cell Culture and Reagents.* Human colon carcinoma (HCT 116), human lung carcinoma (A549), human prostate adenocarcinoma (PC-3), human cervical carcinoma (HeLa), and human embryonic kidney 293T (HEK293T) cells were provided by the Korean Cell Line Bank (KCLB). Human gastric mucosa epithelial (HFE145) cells were received from Dr. Ashktorab (Howard university, USA). Mouse embryonal carcinoma F9−12 cells were kindly supplied by Dr. A. Kihara in Hokkaido University, Japan. The cells were grown in RPMI1640 medium (Hyclone) supplemented with 10% fetal bovine serum (FBS, Invitrogen) and 1% penicillin−streptomycin (Invitrogen). All of the cell lines were incubated at 37 °C under 5% CO_2 in a humidified atmosphere and subcultured once or twice a week. Cells that were passed more than three times were used in the experiments. ER-Tracker Red (BODIPY TR glibenclamide, E34250), Golgi-Tracker (BODIPY TR Ceramide complexed to BSA, B34400), MitoTracker Red (M22425), and LysoTracker Red DND-99 (L7528) were purchased from Invitrogen.

Sulforhodamine B (SRB) Assays.[34,35] The antiproliferative effects of all of the compounds were determined by the SRB assay. Cells were plated in 96-well plates at a density of 5 × 10^4 cells/mL (HCT 116 and PC-3) or 2.5 × 10^4 cells/mL (A549, HEK293T, and HFE145) and incubated for 24 h. The test compounds (dissolved in pure DMSO) were diluted in the medium and the cells were treated for 48 h. The tested cells were then fixed with 10% trichloroacetic acid for 60 min at 4 °C. The fixed cells were stained with 0.4% SRB for 60 min at room temperature. The stained cells were then dissolved in 10 mM Tris buffer (pH 10.0). The absorbance was measured using a microplate reader at 515 nm. The cell survival (%) of each tested group was determined by comparison with solvent-treated control cells. The IC_{50} value, the concentration of 50% cell survival, was estimated by nonlinear regression analysis.

Flow Cytometric Cellular Uptake. HCT 116 cells (1 × 10^6 cells/mL) were plated in 6-well plates and cultured for 24 h. After incubation with the fluorescence probes **4** or **5** (5 μM) for 5 min, the cells were washed twice with phosphate-buffered saline (PBS) and then incubated with 0.05% trypsin for 5 min. The cells were harvested and centrifuged at 1000 rpm for 5 min. The pellet was suspended and washed twice with PBS and finally resuspended for fluorescence analysis using a Beckman Coulter Epics XL Flow Cytometer with a laser excitation of 488 nm.

Confocal Microscopy Analysis. HeLa cells (1 × 10^4 cells/mL) were seeded into 4-well culture slides (SPL, Seoul, Korea) and cultured for 24 h. The cells were initially stained with ER-Tracker Red (1 μM), Golgi-Tracker (10 μM), or MitoTracker Red (1 μM) for 30 min at 37 °C under 5% CO_2. The cells were rinsed twice with PBS and then treated with fluorescence probe **4** (5 μM). At various times (5 min, 10 min, or 15 min) after treatment with probe **4**, the cells were washed three times with PBS and fixed in methanol for 5 min followed by washing of the cells with PBS three times before the confocal imaging analysis. After removal of the 4-well culture slides from the chamber, the slides were mounted for digital micrographs using a LSM 700 ZEISS laser scanning confocal microscope, and then the samples were analyzed by a computer for processing using LSM Colocalization Software. Selected images are representative of at least 3 microscopic fields analyzed for each condition.

Metabolites Analysis by HPLC-FLD. F9−12 cells (1 × 10^6 cells/mL) were seeded into 6-well gelatin coated plates and cultured for 24 h. After incubation with the fluorescence probes **4** or **5** (5 μM) for 60 min, the cells were washed twice with phosphate-buffered saline (PBS) and then were scraped in 0.3 mL of lysis buffer (1 mM PMSF, l × protease inhibitor cocktail, and 1 mM dithiothreitol). The protein concentration of the resulting supernatant was determined by BCA assay. From the cell lysate, 100 μg protein was added to a mixture of MeOH, $CHCl_3$, 1 M HCl, and 1 M NaCl (300:500:30:250 μL, respectively) and then was vigorously vortexed for 30 min and centrifuged at 14 000 rpm. The organic phase was transferred to a fresh tube and dried completely by speed vacuum system (Vision Scientific, Korea). The residues were dissolved in 200 μL of MeOH and then filtered through a 0.45 μm syringe filter before injection into the HPLC system. Samples were separated and analyzed by Agilent 1260 HPLC separation module (Agilent Technologies, Palo Alto, CA, USA) equipped with a Waters Sunfire (150 mm × 4.6 mm, 5 μm, Waters, USA) column and Agilent 1260 Infinity fluorescence detector. The detection wavelengths were set at 485 nm for excitation and 538 nm for emission, respectively. The injection volume of the samples was 10 μL. The separation was performed at 40 °C, with a flow rate of 1 mL/min using a mobile phase composed of H_2O with 0.1% triethyamine (v/v) (A) and MeOH with 0.1% triethylamine (v/v) (B). The following optimized elution program was applied to separate cellular probes **4** or **5** and other metabolites: 50% B, 0−2 min; 50% B to 100% B, 2−10 min; 100% B, 10−15 min; 100% B to 50% B, 15−15.5 min; 50% b, 15.5−20 min. The eluted probes **4** and **5** peaks were identified by each corresponding standard compound.

Metabolite Analysis by LC-MS. Probe **4** metabolites were analyzed by a Surveyor HPLC instrument (Thermo Scientific, USA) coupled directly to ion trap mass spectrometer (Thermo scientific, USA). The chromatographic separation was performed at room temperature on Luna C18 column (150 mm × 2.0 mm, 5 μm, Phenomenex, USA). The mobile phase composed of 1 mM ammonium formate in water with 0.2% formic acid (v/v) (A) and 2 mM ammonium formate in MeOH with 0.2% formic acid (v/v) (B), delivered at a flow rate of 300 μL/min. The gradient elution program was as follows: 50% B, 0−0.5 min; 50% B to 100% B, 0.5−8 min; 100% B, 8−24 min; 100% B to 50% B, 24−25 min; 50% b, 25−35 min. The total run time for each injection was 35 min and the injection volume was 10 μL. The mass spectrometer was operated in positive ion mode with an ESI source. Instrument control, data acquisition, and data analysis were performed by Xcalibur 2.1 software (Thermo Scientific, USA). Helium and N_2 gas were used for collision and desolvation gas and heating and nebulizing gas, respectively. The other ionization parameters were as follows: auxiliary gas, 12 psi; nebulizing gas, 2 psi; sheath gas, 2 psi; source temperature, 275 °C; electron voltage, 4.5 kV. The SIM transitions were (m/z) 548.3, 762.3, 790.3, 816.4, and 818.4.

■ RESULTS AND DISCUSSION

Antiproliferative Activities of Polyyne-Containing Sphingoid Bases. The typical biological activities of sphingoid bases include antiproliferative activity and apoptosis in cancer cells.[16,17,36,37] Thus, in our preliminary evaluation, we examined the antiproliferative activities of polyyne-sphingosines **2** and **3**. As shown in Table 1, all of the tested polyyne-sphingosines except **2a** were found to be more effective than sphingosine **1**. The observed data revealed that the potency against cancer cell lines was highly dependent on the composition of the polyyne-sphingosines. In general, the $\Delta^{4,5}$-triple bond compounds **3**

Table 1. Antiproliferative Effects for Polyyne-Containing Sphingoid Base Analogues

compound	IC_{50} [μM][a]	
	HCT116[b]	A549[c]
sphingosine **1**	6.76	>10
2a (n = 1)	6.98	>10
2b (n = 2)	2.43	6.86
2c (n = 3)	1.34	4.75
3a (n = 1)	0.66	2.67
3b (n = 2)	0.14	1.20
3c (n = 3)	0.11	0.25

[a]All values are the means of a minimum of three experiments. [b]Human colon carcinoma. [c]Human lung carcinoma.

Table 2. Antiproliferative Effects of Sphingoid Base Probes 4 and 5 against Human Cell Lines

compound	IC_{50} [μM][a]				
	HCT116[b]	A549[c]	PC-3[d]	HEK293T[e]	HFE-145[f]
NBD-triyne-sphingosine **4**	0.22	5.60	0.70	15.2	12.8
NBD-sphingosine **5**	25.6	>50	40.5	10.4	12.5

[a]All values are the means of a minimum of three experiments. [b]Human colon carcinoma. [c]Human lung carcinoma. [d]Human prostate adenocarcinoma. [e]Human embryonic kidney. [f]Human gastric mucosa epithelial.

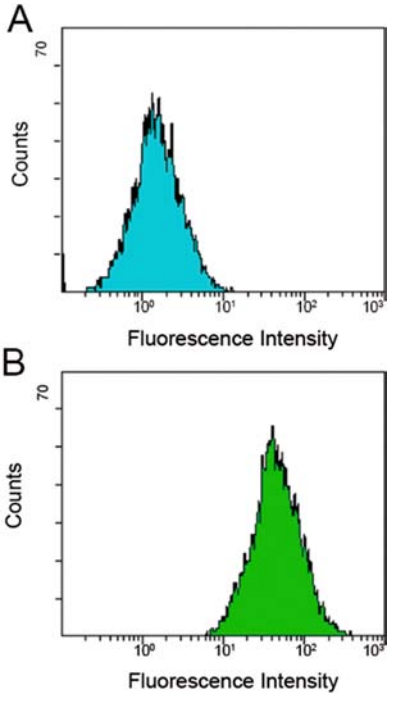

Figure 2. Flow cytometric analysis of the cellular uptake of 5 μM of NBD-sphingosine **5** (A) and NBD-triyne-sphingosine **4** (B) by HCT116 human colon cancer cells (10^6 cells per sample) after incubation for 5 min at 37 °C.

were approximately ten times more potent than the corresponding $\Delta^{4,5}$-double bond compounds **2**. In addition, it was found that a higher number of acetylene units elicited higher activity. The most potent compound was tetrayne **3c**

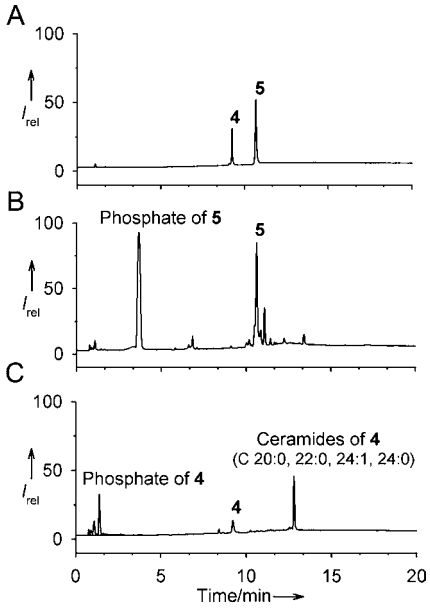

Figure 3. HPLC-FLD chromatograms. Standard chromatogram of probes **4** and **5** (A). Chromatograms of the lipid extracts from F9–12 cells incubated with 5 μM of fluorescence probe **5** (B) or probe **4** (C) for 60 min at 37 °C.

with IC_{50} values of 0.11 and 0.25 μM against HCT116 and A549 cells, respectively.

Design and Synthesis of NBD-triyne-sphingosine 4. The covalent attachment of fluorescent dyes to bioactive molecules is a popular method for visual monitoring of the behavior of molecules and provides a useful chemical tool for studying biological events within cells.[38,39] However, the attached fluorophore often leads to undesired effects on the probe's binding affinity, cell permeability, and biological activity. Taking this into consideration, we surveyed some common fluorescent dyes and selected the NBD-group as the fluorescent probe. NBD was chosen because of its favorable fluorescence properties and compact size. Moreover, it displays environmentally sensitive fluorescence—weak fluorescence in water and strong fluorescence in hydrophobic environments, including membranes and enzyme binding sites.[33,40−42] This convenient property is especially useful for sphingoid base probes because sphingolipids exert their effects either through specific binding to enzymes or through hydrophobic interactions with other membrane components.[1,43,44] In fact, a number of NBD-labeled sphingolipids have been synthesized and utilized.[24−33]

Although the most potent compound from our polyyne-sphingosine series was tetrayne-sphingosine **3c**, we selected triyne-sphingosine **3b** as a platform to design our polyyne-sphingosine fluorescent probe because tetrayne **3c** was found to be less stable than triyne **3b** at room temperature. The fluorescently labeled triyne-sphingosine **4** was designed with an NBD group at the end of the alkyl chain and an NH group as the linker. The alkyl chains in this derivative are 18 carbons in length, identical to that of natural sphingosine.

Scheme 1 depicts an outline of our synthesis of target compound **4**. The cross-coupling of bromodiyne **6** with terminal acetylene **7** was the key step in this synthesis. Bromodiyne **6** was obtained from commercially available (*S*)-Garner's aldehyde **8**[45] via a conventional five-step sequence according to our previously reported procedure.[22] NBD-

dx.doi.org/10.1021/bc300684q | *Bioconjugate Chem.* 2013, 24, 1324−1331

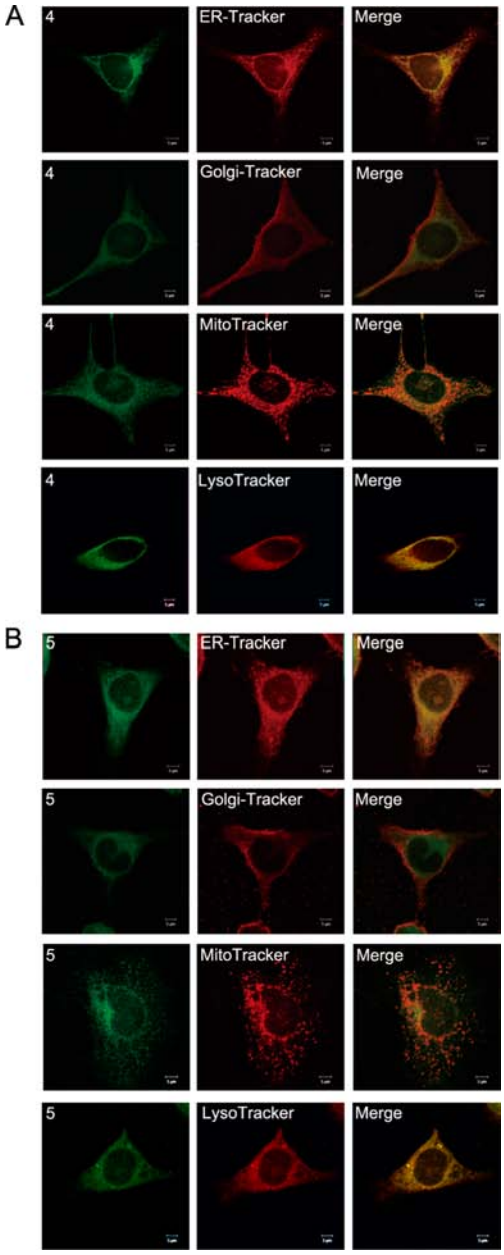

Figure 4. Subcellular localization of NBD-triyne-sphingosine **4** (green) (A) and NBD-sphingosine **5** (green) (B) followed by time to progression in HeLa cells (10^4 cells per sample) monitored with each tracker (red). Cells were stained with 1 μM ER-Tracker Red, 10 μM Golgi-Tracker Red, 1 μM MitoTracker Red, or 100 nM LysoTracker Red DND-99 at 37 °C for 30 min. The cells were incubated with 5 μM of probes **4** or **5** for 15 min. The merged color images show each probe incorporated into the ER, Golgi, mitochondria, and lysosome of HeLa cells. The scale bar represents 5 μm.

containing terminal acetylene **7** was prepared from ω-bromo acid **9** in five steps. The nucleophilic addition of acetylide to bromide **9** gave acetylenic product **10**. The carboxylic acid group of **10** was transformed into the corresponding primary amine to give **11**. Reaction of amine **11** with NBD-Cl followed by removal of the silyl protecting group provided terminal acetylene **7**, which was cross-coupled with bromodiyne **6** using modified Sonogashira conditions to give triyne **12** in 59% yield. Finally, removal of all of the protecting groups in **12** furnished the desired NBD-triyne-sphingosine **4**. Fortunately, this fluorescent compound was stable in a normal laboratory atmosphere. The fluorescence quantum yield of **4** was 0.13 in DMSO solution,[46] and its fluorescence was strongly dependent on the polarity of the solvent like that of other NBD derivatives (see Supporting Information, Figure S1).[47]

Antiproliferative Activities of NBD-triyne-sphingosine 4. To determine whether the NBD label significantly affects the antiproliferative activities of polyyne-sphingosines, the potency of **4** was examined (Table 2). NBD-triyne-sphingosine **4** was slightly less potent than the corresponding triyne-sphingosine **3b**. For example, the IC_{50} value of **4** against HCT116 cells was 0.22 μM, while that of **3b** was 0.14 μM. These data indicated that the NBD label causes adverse effects, but they are not significant. NBD-triyne-sphingosine **4** was found to be much more effective than sphingosine **1** and NBD-sphingosine **5** in inhibiting cancer cell growth. Antiproliferative effects of **4** and **5** on normal human cell lines were also examined by using HEK239T and HFE-145. Fluorescence probe **4** was substantially less cytotoxic toward normal human cells. Interestingly, cytotoxicity of **5** toward normal cells was very similar to that of **4**, although their potencies were significantly different in cancer cells.

NBD-triyne-sphingosine 4 Uptake by Cultured Cells. To understand the possible mechanisms or factors responsible for the higher antiproliferative effect of **4** on cancer cells, a flow cytometric analysis was performed for fluorescence probes **4** and **5**. As shown in Figure 2, HCT116 human colon cancer cells fed with probe **4** for 5 min showed significantly increased fluorescence intensity compared with the probe **5** treated cells. This result indicated that NBD-triyne-sphingosine **4** was more readily incorporated into the cells than was NBD-sphingosine **5**, at least within the time frame used for our experiments. Thus, one highly possible explanation for the higher antiproliferative activity of **4** could be an increase in cell permeability. In general, more lipophilic compounds have greater permeability. However, the improved translocation of **4** into the cells was most likely due to its more rigid polyyne structure rather than its lipophilicity because the ALog P value of **4** was lower than that of **5** (4.54 vs 5.06).

The significantly higher fluorescence intensity observed in the flow cytometric analysis could also be explained by an increased hydrophobic environment around the NBD fluorophore.[25,33] In other words, NBD-triyne-sphingosine **4** might be more efficiently bound to membranes or hydrophobic clefts in the enzymes than was NBD-sphingosine **5**. Thus, another possible explanation for the higher antiproliferative activity of **4** is its novel or enhanced biological properties presumably resulting from the presence of its polyyne moiety.

Metabolism of NBD-triyne-sphingosine 4. To further understand the enhanced antiproliferative activity of polyyne-containing sphingoid base, the metabolism of NBD-triyne-sphingosine **4** and NBD-sphingosine **5** was studied. In these experiments, we used F9−12 cells that lack S1P lyase and stably express Sphk1. Each probe was incubated with cells for 1 h and the resulting metabolites were analyzed by HPLC and LC-MS. As shown in Figure 3, NBD-sphingosine **5** was converted mostly to the corresponding phosphate. On the other hand, NBD-triyne-sphingosine **4** exhibited a different pattern of metabolism. The chromatogram of metabolites of **4** showed two dominant peaks. The molecular mass of the first peak (1.4 min) in the elution profile corresponded to that of the phosphate form. The MS/MS analysis of the peak at 12.8 min (see Supporting Information, Figure S2) indicated that NBD-

dx.doi.org/10.1021/bc300684q | Bioconjugate Chem. 2013, 24, 1324−1331

triyne-sphingosine **4** was also metabolized to NBD-triyne ceramides having various fatty acyl chain lengths ($C_{20:0}$, $C_{22:0}$, $C_{24:1}$, and $C_{24:0}$). These metabolic differences may be one of the explanations for why polyyne-containing sphingoid base showed more antiproliferative activity.

Visualization of Cellular Uptake of NBD-triyne-sphingosine 4. To visualize the uptake of NBD-triyne-sphingosine **4** and NBD-sphingosine **5** in living cells, HeLa cells were incubated with 5 μM of probes at 37 °C. The endoplasmic reticulum (ER), Golgi, mitochondria, and lysosome of the cells were visibly labeled by ER-Tracker, Golgi-Tracker, MitoTracker, and LysoTracker, respectively. We fixed the probe-treated cells and imaged them using a confocal laser scanning microscope. Both fluorescence probes **4** and **5** were rapidly incorporated into the cells within 5 min after treatment, and they showed a similar cellular distribution pattern. The confocal image showed broad cytoplasmic distribution of the probes and their clear separation from the nucleus. Both fluorescence probes did not display a clearly polarized distribution in the intracellular organelles, even after longer (15 min) incubation (Figure 4 and Figure S3).

CONCLUSION

Although much research has been performed on sphingolipids over the last two decades, there are still many important questions that remain unanswered about the detailed functions and mechanisms of these compounds. To better understand the biological and biophysical roles of sphingolipids, chemical tools with unique biological and physicochemical properties are needed. In this regard, we presented a polyyne-containing sphingoid base and its fluorescently labeled (NBD) derivative that are much more effective than either the parent sphingosine or NBD-sphingosine in inhibiting cancer cell growth. Cells fed with NBD-triyne-sphingosine **4** showed a significantly increased fluorescence signal compared with those fed with NBD-sphingosine **5**. One explanation is that the rigid polyyne moiety might enable the compound to pass through cell membranes more readily. Another possible explanation is that NBD-triyne-sphingosine **4** was more readily attracted to the hydrophobic regions of the cells, such as the membranes or binding sites in enzymes. Although more systematic studies are needed to clearly elucidate the origin of the increase in fluorescence intensity and the higher antiproliferative activity of **4**, these properties are some of the interesting and distinct aspects of NBD-triyne-sphingosine **4** compared to normal NBD-sphingosine probes. Based on these initial results, fluorescently labeled polyyne-containing sphingoid base **4** will represent a useful chemical tool for sphingolipid research.

ASSOCIATED CONTENT

Supporting Information

The method for determining the quantum yield for compound **4**, Figure S1, Figure S2, Figure S3, and copies of ^{1}H and ^{13}C NMR spectra for selected compounds (**7**, **12**, and **4**). This material is available free of charge via the Internet at http://pubs.acs.org.

AUTHOR INFORMATION

Corresponding Author

*Tel: 82-2-880-2487. Fax: 82-2-888-0649. E-mail: pennkim@snu.ac.kr.

Author Contributions

Y.M.L. and C.L. contributed equally to this work.

Notes

The authors declare no competing financial interest.

ACKNOWLEDGMENTS

This work was supported by SRC/ERC program (R11-2007-107-02001-0) and WCU program (R32-2008-000-10098-0) through KOSEF funded by MEST.

REFERENCES

(1) Hannun, Y. A., and Obeid, L. M. (2008) Principles of bioactive lipid signaling: lessons from sphingolipids. *Nat. Rev. Mol. Cell. Biol. 9*, 139−150.

(2) Bartke, N., and Hannun, Y. A. (2009) Bioactive sphingolipids: metabolism and function. *J. Lipid Res. 50*, S91−S96.

(3) Hla, T., and Dannenberg, A. J. (2012) Sphingolipid signaling in metabolic disorders. *Cell Metab. 16*, 420−434.

(4) Cuvillier, O., Pirianov, G., Kleuser, B., Vanek, P. G., Coso, O. A., Gutkind, J. S., and Spiegel, S. (1996) Suppression of ceramide-mediated programmed cell death by sphingosine-1-phosphate. *Nature 381*, 800−803.

(5) Fyrst, H., and Saba, J. D. (2010) An update on sphingosine-1-phosphate and other sphingolipid mediators. *Nat. Chem. Biol. 6*, 489−497.

(6) Maceyka, M., Milstien, S., and Spiegel, S. (2009) Sphingosine-1-phosphate: the Swiss army knife of sphingolipid signaling. *J. Lipid Res. 50*, S272−S276.

(7) Obeid, L. M., Linardic, C. M., Karolak, L. A., and Hannun, Y. A. (1993) Programmed cell death induced by ceramide. *Science 259*, 1769−1771.

(8) Pettus, B. J., Chalfant, C. E., and Hannun, Y. A. (2002) Ceramide in apoptosis: an overview and current perspectives. *Biochim. Biophys. Acta 1585*, 114−125.

(9) Taha, T. A., Mullen, T. D., and Obeid, L. M. (2006) A house divided: Ceramide, sphingosine, and sphingosine-1-phosphate in programmed cell death. *Biochim. Biophys. Acta 1758*, 2027−2036.

(10) Gandy, K. A. O., and Obeid, L. M. (2013) Targeting the sphingosine kinase/sphingosine 1-phosphate pathway in disease: Review of sphingosine kinase inhibitors. *Biochim. Biophys. Acta 1831*, 157−166.

(11) Pitson, S. M. (2011) Regulation of sphingosine kinase and sphingolipid signaling. *Trends Biochem. Sci. 36*, 97−107.

(12) Shida, D., Takabe, K., Kapitonov, D., Milstien, S., and Spiegel, S. (2008) Targeting SphK1 as a new strategy against cancer. *Curr. Drug Targets 9*, 662−673.

(13) Ogretmen, B., and Hannun, Y. A. (2004) Biologically active sphingolipids in cancer pathogenesis and treatment. *Nat. Rev. Cancer 4*, 604−616.

(14) Spiegel, S., and Milstien, S. (2011) The outs and the ins of sphingosine-1-phosphate in immunity. *Nat. Rev. Immunol. 11*, 403−415.

(15) Chigorno, V., Giannotta, C., Ottico, E., Sciannamblo, M., Mikulak, J., Prinetti, A., and Sonnino, S. (2005) Sphingolipid uptake by cultured cells. *J. Biol. Chem. 280*, 2668−2675.

(16) Cuvillier, O. (2002) Sphingosine in apoptosis signaling. *Biochim. Biophys. Acta 1585*, 153−162.

(17) Suzuki, E., Handa, K., Toledo, M. S., and Hakomori, S. (2004) Sphingosine-dependent apoptosis: A unified concept based on multiple mechanisms operating in concert. *Proc. Natl. Acad. Sci. U.S.A. 101*, 14788−14793.

(18) Gangoiti, P., Camacho, L., Arana, L., Ouro, A., Granado, M. H., Brizuela, L., Casas, J., Fabriás, G., Abad, J. L., Delgado, A., and Gómez-Muñoz, A. (2010) Control of metabolism and signaling of simple bioactive sphingolipids: Implications in disease. *Prog. Lipid Res. 49*, 316−334.

(19) Pruett, S. T., Bushnev, A., Hagedorn, K., Adiga, M., Haynes, C. A., Sullards, M. C., Liotta, D. C., and Merrill, A. H., Jr. (2008)

Biodiversity of sphingoid bases ("sphingosines") and related amino alcohols. *J. Lipid Res. 49*, 1621−1639.
(20) Delgado, A., Casas, J., Llebaria, A., Abad, J. L., and Fabrias, G. (2007) Chemical tools to investigate sphingolipid metanolism and functions. *ChemMedChem 2*, 580−606.
(21) Menaldino, D. S., Bushnev, A., Sun, A., Liotta, D. C., Symolon, H., Desai, K., Dillehay, D. L., Peng, Q., Wang, E., Allegood, J., Trotman-Pruett, S., Sullards, M. C., and Merrill, A. H., Jr. (2003) Sphingoid bases and de novo ceramide synthesis: enzymes involved, pharmacology and mechanisms of action. *Pharmacol. Res. 47*, 373−381.
(22) Kim, S., Lee, Y. M., Kang, H. R., Cho, J., Lee, T., and Kim, D. (2007) Synthesis of novel polyyne analogues of sphingoid base via an iterative acetylene homologation sequence. *Org. Lett. 9*, 2127−2130.
(23) Nakayama, S., Uto, Y., Tanimoto, K., Okuno, Y., Sasaki, Y., Nagasawa, H., Nakata, E., Arai, K., Momose, K., Fujita, T., Hashimoto, T., Okamoto, Y., Asakawa, Y., Goto, S., and Hori, H. (2008) TX-2152: A conformationally rigid and electron-rich diyne analogue of FTY720 with in vivo antiangiogenic activity. *Bioorg. Med. Chem. 16*, 7705−7714.
(24) Hakogi, T., Shigenari, T., Katsumura, S., Sano, T., Kohno, T., and Igarashi, Y. (2003) Synthesis of fluorescence-labeled sphingosine and sphingosine-1-phosphate; Effective tools for sphingosine and sphingosine-1-phosphate behavior. *Bioorg. Med. Chem. Lett. 13*, 661−664.
(25) Billich, A., and Ettmayer, P. (2004) Fluorescence-based assay of sphingosine kinases. *Anal. Biochem. 326*, 114−119.
(26) Ettmayer, P., Billich, T., Mechtcheriakova, D., Schmid, H., and Nussbaumer, P. (2004) Fluorescence-labeled sphingosines as substrates of sphingosine kinases 1 and 2. *Bioorg. Med. Chem. Lett. 14*, 1555−1558.
(27) Nussbaumer, P., Ettmayer, P., Peters, C., Rosenbeiger, D., and Högenauer, K. (2005) One-step labeling of sphingolipids *via* a scrambling cross-metathesis reaction. *Chem. Commun.*, 5086−5087.
(28) Peters, C., Billich, A., Ghobrial, M., Högenauer, K., Ullrich, T., and Nussbaumer, P. (2007) Synthesis of borondipyrromethene (BODIPY)-labeled sphingosine derivatives by cross-metathesis reaction. *J. Org. Chem. 72*, 1842−1845.
(29) Ettmayer, P., Baumruker, T., Guerini, D., Mechtcheriakova, D., Nussbaumer, P., Streiff, M. B., and Billich, A. (2006) NBD-labeled derivatives of the immunomodulatory drug FTY720 as tools for metabolism and mode of action studies. *Bioorg. Med. Chem. Lett. 16*, 84−87.
(30) Nussbaumer, P. (2008) Medicinal chemistry aspects of drug targets in sphingolipid metabolism. *ChemMedChem 3*, 543−551.
(31) Bedia, C., Camacho, L., Casas, J., Abad, J. L., Delgado, A., Van Veldhoven, P. P., and Febriàs, G. (2009) Synthesis of a fluorogenic analogue of sphingosine-1-phosphate and its use to determine sphingosine-1-phosphate lyase activity. *ChemBioChem 10*, 820−822.
(32) Kim, R., Lou, K., and Kraft, M. L. (2013) A new, long-wavelength borondipyrromethene sphingosine for studying sphingolipid dynamics in live cells. *J. Lipid Res. 54*, 265−275.
(33) Haldar, S., and Chattopadhyay, A. (2013) Application of NBD-labeled lipids in membrane and cell biology. *Springer Series on Fluorescence* (Mely, Y., and Duportail, G., Eds.) pp 37−50, Vol *13*, Springer, Heidelberg.
(34) Shehan, P., Storeng, R., Scudiero, D., Monks, A., McMahon, J., Vistica, D., Warren, J. T., Bokesch, H., Kenney, S., and Boyd, M. R. (1990) New colorimetric cytotoxicity assay for anticancer-drug screening. *J. Natl. Cancer Inst. 82*, 1107−1112.
(35) Vichai, V., and Kirtikara, K. (2006) Sulforhodamine B colorimetric assay for cytotoxicity screening. *Nat. Protoc. 1*, 1112−1116.
(36) Nagahara, Y., Shinomiya, T., Kuroda, S., Kaneko, N., Nishio, R., and Ikekita, M. (2005) Phytosphingosine induced mitochondria-involved apoptosis. *Cancer Sci. 96*, 83−92.
(37) Ahn, E. H., and Schroeder, J. J. (2002) Sphingoid bases and ceramide induce apoptosis in HT-29 and HCT-116 human colon cancer cells. *Exp. Biol. Med. 227*, 345−353.
(38) McGrath, J. C., Arribas, S., and Daly, C. J. (1996) Fluorescent ligands for the study of receptors. *Trends Pharmacol. Sci. 17*, 393−399.
(39) Daly, C. J., and McGrath, J. C. (2003) Fluorescent ligands, antibodies, and proteins for the study of receptors. *Pharmacol. Ther. 100*, 101−118.
(40) Mazeres, S., Schram, V., Tocanne, J.-F., and Lopez, A. (1996) 7-Nitrobenz-2-oxa-1,3-diazole-4-yl-labeled phospholipids in lipid membranes: differences in fluorescence behavior. *Biophys. J. 71*, 327−335.
(41) Fery-Forgues, S., Fayet, J.-P., and Lopez, A. (1993) Drastic changes in the fluorescence properties of NBD probes with the polarity of the medium: involvement of a TICT state? *J. Photochem. Photobiol., A 70*, 229−243.
(42) Taliani, S., Simorini, F., Sergianni, V., Motta, C. L., Settimo, F. D., Cosimelli, B., Abignente, E., Greco, G., Novellino, E., Rossi, L., Gremigni, V., Spinetti, F., Chelli, B., and Martini, C. (2007) New fluorescent 2-phenylindolglyoxylamide derivatives as probes targeting the peripheral-type benzodiazepine receptor: design, synthesis, and biological evaluation. *J. Med. Chem. 50*, 404−407.
(43) Contreras, F.-X., Sot, J., Alonso, A., and Goni, F. M. (2006) Sphingosine increases the permeability of model and cell membranes. *Biophys. J. 90*, 4085−4092.
(44) van Meer, G., Voelker, D. R., and Feigenson, G. W. (2008) Membrane lipids: where they are and how they behave. *Nat. Rev. Mol. Cell Biol. 9*, 112−124.
(45) Garner, P., and Park, J. M. (1998) *Organic Syntheses*, pp 300−305, Collect. Vol. *IX*, Wiley, New York.
(46) The fluorescence quantum yield of **4** was determined using anthracene in ethanol as a reference.
(47) Mukherjee, S., Chattopadhyay, A., Samanta, A., and Soujanya, T. (1994) Dipole moment change of NBD group upon excitation studied using solvatochromic and quantum chemical approaches: Implications in membrane research. *J. Phys. Chem. 98*, 2809−2812.